

High R_1 of Mn^{2+} adsorbed to hydrophilic pores of magnetoferritin nanoparticles

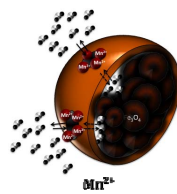
V. Clavijo Jordan¹, and K. M. Bennett¹

¹School of Biological and Health Systems Engineering, Arizona State University, Tempe, AZ, United States

Introduction: Increasing the relaxivity of MRI contrast agents is critical to the development of useful preclinical and clinical molecular MRI probes. Proton relaxation enhancement due to the presence of paramagnetic ions is sensitive to the rate of exchange of protons between the agent and the bulk water (1). Previous studies have shown large (~10-fold) increases in per-ion T_1 relaxivity (R_1) in a lanthanide chelate due to binding with bovine serum albumin (2), and a similar strong enhancement has been observed in Gd-doped carbon nanotubes (3). Here we report a surprisingly large increase in R_1 when paramagnetic Mn^{2+} is adsorbed in the hydrophilic channels of iron-filled ferritin (magnetoferritin) nanoparticles (4). We synthesized a magnetoferritin- Mn^{2+} complex with a per-ion R_1 of $330\text{mM}^{-1}\text{s}^{-1}$, attributed primarily to the Mn^{2+} incorporation. We used electron spin resonance (ESR) to confirm that manganese did not interact with the iron core, but was rather incorporated into the protein surface hydrophilic channels. The strong increase in R_1 by ionic adsorption leads to the possibility of enhancing relaxation in ferritin and other synthetic agents by strategic placement of paramagnetic ions relative to exchanging water.

Methods: Particle Synthesis: To create ferritin with manganese adsorbed to surface hydrophilic channels, $2\mu\text{M}$ Apoferritin (Sigma Aldrich) buffered in 0.05M MES at pH 8.5, 48mM Fe(II)Chloride (Sigma Aldrich) and 4.8mM Mn(II)Chloride (Sigma Aldrich) were de-aerated for 20 minutes with N_2 (50psi). The solution was kept at 55 to 60°C . We added $125\mu\text{L}$ of $MnCl_2$ and $125\mu\text{L}$ of $FeCl_2$ in sequence to the apoferritin solution. We made a total of 12 and 8 additions of $MnCl_2$ and $FeCl_2$. Samples were dialyzed against 0.15M NaCl, and filtered using a magnetic column (Milttenyi Biotec), eluted into 0.15M NaCl buffer. As a control, $2\mu\text{M}$ bovine serum albumin (Thermo Scientific) was used instead of apoferritin. Total protein concentration was obtained with a Bradford assay, and inductively coupled plasma – optical emission spectroscopy (ICP-OES) was used to measure metal concentrations. Relaxometry: Relaxivity was measured using a 1.5T Bruker Minispec relaxometer. Bruker's curve-fitting tool was used find the corresponding T_2 values (Inter pulse $\tau = 10\text{ms}$, 200 points) and T_1 values (pulse separations ranging from 5 to 20000ms , 4 scans, 10 points) of samples suspended in a 1% agarose gel. Electron Microscopy: Samples were adsorbed on Cu-C grids and transmission electron microscopy (TEM) images were obtained using a Philips CM12 electron microscope. High Resolution Electron Microscopy (HREM) images were obtained using a Philips CM200-FEG TEM/STEM. Fast Fourier Transform patterns of the HRTEM images were obtained from 4 different particles and analyzed using ImageJ software (NIH). Native Gel Electrophoresis: Samples were buffered in Native Tris-Glycine Sample Buffer (Invitrogen). $10\mu\text{L}$ of native ferritin, apoferritin, or Mn^{2+} loaded magnetoferritin were loaded into wells of a 4 - 20% Tris-glycine gel. The gel ran for 4 hours at of 125V and 6 - 12mA /gel. Gels were stained for 1h with Simply Blue (Invitrogen). Electron Spin Resonance: EPR was performed with a X-band spectrometer (Bruker ESP300E) with 1mW power, 30G modulation and at 5K under liquid helium.

Results and Conclusions: The addition of Mn^{2+} to the synthesis of magnetoferritin can enhance the per-ion and per-particle relaxivity above typical values, as shown in the table of Figure 1. Interestingly, this per-particle and per-ion relaxivity enhancement was only accomplished when the particle was iron-loaded and magnetically filtered, and only when Mn^{2+} was incorporated in the ferritin. Electron microscopy (TEM and HREM) showed that highly electron dense cores (4 - 6nm) were obtained only with apoferritin, as BSA formed amorphous crystals (data not shown) Figure 2a,b. Crystalline metallic cores were found in HREM with lattice spacings of 2.5\AA , which corresponds to magnetite (Figure 2d,f). Native gel electrophoresis showed that the protein structure was maintained intact after synthesis since our agent showed bands of the same molecular weight as apoferritin, and native ferritin (Figure 2e). EPR showed that Fe(II) gets converted to Fe(III) during the last steps of synthesis and that the addition of Mn^{2+} did not affect the formation of Fe(III) in the cores (data not shown). EPR of our agent compared to $MnCl_2$ in water indicated that Mn^{2+} is coordinated to a matrix and not free in solution; also, the characteristic 6-peak splitting of the Mn^{2+} signal at 3000G (g-factor = 2.0) and 90G hyperfine lines of Mn^{2+} - Mn^{2+} interactions of less than 5\AA were present (5). It has been shown that apoferritin has increased affinity to some metal ions, which compete for binding sites in the protein's surface channels (6) where we suspect our Mn^{2+} ions are clustered. Others have shown that apoferritin has a catalytic effect on the exchange of protons located in the interior of the protein's cavity, dramatically increasing the lanthanide relaxivity (7). We hypothesize that a similar effect occurs in our synthesis, and that the paramagnetic Mn^{2+} ions hinder water exchange through the pores, thus maintaining the inner core water molecules to a confined space between catalytic inner core residues and iron oxide crystal. We conclude that R_1 may be dramatically increased by the strategic placement of paramagnetic ions within the pores of apoferritin and other synthetic contrast agents.



	R_2 $\text{mM}^{-1}\text{s}^{-1}$	R_1 $\text{mM}^{-1}\text{s}^{-1}$	R_2/R_1
Fe	133	1.15	115.6
Mn	31,112	338.6	91.8
Particle	222,481	2774	80.2
Volumetric / nm^3	193.40	2.41	80.2
Fe	78	0.07	1114.0
Particle	404,045	407	992.7
Magnetoferritin particles	351.23	0.35	1003.5
Volumetric / nm^3			

Figure 1. Mn^{2+} magnetoferritin particle, and pure magnetoferritin particle relaxivities based on iron, particle concentrations and volume of particle. For transverse (R_2) and longitudinal (R_1) relaxivities a CPMG and an IR pulse sequence was used respectively. Schematic showing the suspected water interaction through the particle pores and the iron oxide crystal (top schematic).

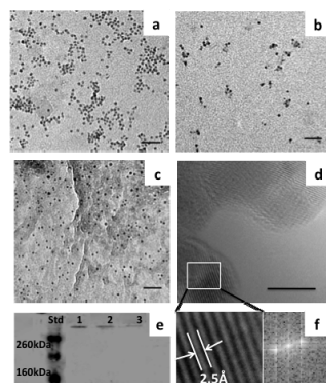


Figure 2. TEM images of (a) Native ferritin, (b) Mn^{2+} magnetoferritin, (c) Magnetoferritin. Scale bars are 50nm (d) HREM of Mn^{2+} magnetoferritin showing lattice fringes (scale bar is 5nm). (e) Native gel of (1) apoferritin, (2) native ferritin, and (3) Mn^{2+} magnetoferritin. (f) FFT and inverse FFT of ROI confirm the presence of magnetite in the apoferritin cores (lattice spacing = 2.5\AA)

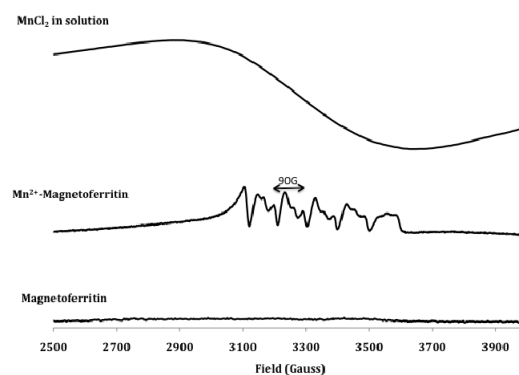


Figure 3. EPR Spectrum of $MnCl_2$ in dH_2O showing no coordination to a matrix (top). Mn^{2+} magnetoferritin showing characteristic hyperfine lines of 90G and g-factor 2.0 (middle). Magnetoferritin showing no Mn^{2+} signal (bottom).

References: (1) Burtea C. et al. Molecular Imaging I. Handbook of Experimental Pharmacology 185/I. (2008) (2) Caravan P. et al. Inorg. Chem. (2001) 40. 6580-6587 (3) Sitharaman B. et al. Chem. Comm. (2005) 31:3915-3917. (4) Bulte JW. et al. J Magn Reson Imaging (1994);4:497-505 (5) Chae MY. et al. J. Am. Chem. Soc (1993), 115, 12173-12174 (6) Wardeska JG. et al. The Journal of Biological Chemistry. (1986), 261, No.15, 6677-6683. (7) Vasalatiy O. et al. Contrast. Med. Mol. Imaging 1:10-14 (2006).